Stretching our understanding of C_3: Experimental and theoretical spectroscopy of highly excited $nv_1 + mv_3$ states ($n \leq 7$ and $m \leq 3$)

Benjamin Schröder, Kirstin D. Doney, Peter Sebald, Dongfeng Zhao, and Harold Linnartz

Citation: The Journal of Chemical Physics **149**, 014302 (2018); doi: 10.1063/1.5034092
View online: https://doi.org/10.1063/1.5034092
View Table of Contents: http://aip.scitation.org/toc/jcp/149/1
Published by the American Institute of Physics

Stretching our understanding of C_3: Experimental and theoretical spectroscopy of highly excited $n\nu_1 + m\nu_3$ states ($n \leq 7$ and $m \leq 3$)

Benjamin Schröder,[1] Kirstin D. Doney,[2,a)] Peter Sebald,[1] Dongfeng Zhao,[3] and Harold Linnartz[2]

[1]*Universität Göttingen, Institut für Physikalische Chemie, Göttingen D-37077, Germany*
[2]*Sackler Laboratory for Astrophysics, Leiden Observatory, Leiden University, P.O. Box 9513, 2300 RA Leiden, The Netherlands*
[3]*CAS Center for Excellence in Quantum Information and Quantum Physics and Hefei National Laboratory for Physical Sciences at the Microscale, University of Science and Technology of China, Hefei, Anhui, People's Republic of China*

(Received 9 April 2018; accepted 6 June 2018; published online 2 July 2018)

We present the high resolution infrared detection of fifteen highly vibrationally excited $n\nu_1 + m\nu_3$ combination bands ($n \leq 7$ and $m \leq 3$) of C_3 produced in a supersonically expanding propyne plasma, of which fourteen are reported for the first time. The fully resolved spectrum, around 3 μm, is recorded using continuous wave cavity ring-down spectroscopy. A detailed analysis of the resulting spectra is provided by ro-vibrational calculations based on an accurate local *ab initio* potential energy surface for C_3 ($\tilde{X}^1\Sigma_g^+$). The experimental results not only offer a significant extension of the available data set, extending the observed number of quanta v_1 to 7 and v_3 to 3, but also a vital test to the fundamental understanding of this benchmark molecule. The present variational calculations give remarkable agreement compared to experimental values with typical accuracies of ~0.01% for the vibrational frequencies and ~0.001% for the rotational parameters, even for high energy levels around 10 000 cm^{-1}. *Published by AIP Publishing.* https://doi.org/10.1063/1.5034092

I. INTRODUCTION

The linear carbon chain C_3 ($\tilde{X}^1\Sigma_g^+$) is an abundant species in combustion processes and has been identified in different astronomical environments.[1–11] Compared to other pure carbon chains with an odd number of carbon atoms (cf. Ref. 12 and references therein), C_3 is very "floppy," as seen by the extremely low lying bending vibrational frequency (ν_2) at 63 cm^{-1}.[13] As such, C_3 also serves as a benchmark molecule for quantum chemistry.[14–18] Since its discovery in the tail of a comet[1] and subsequent laboratory identification[19] and analysis,[20] C_3 has become one of the most studied triatomic transients.

Most astronomical observations of C_3 have been made through its optical $\tilde{A}^1\Pi_u \leftarrow \tilde{X}^1\Sigma_g^+$ spectrum at 4050 Å. These detections vary from emission spectra in cometary tails to the absorption spectra in diffuse interstellar clouds. More recently, an extensive study, performed with the Very Large Telescope,[11] reported a large number of additional rovibronic C_3 bands involving excited vibrational levels in the $\tilde{A}^1\Pi_u$ state that could be assigned following their laboratory identification.

The first high resolution infrared (IR) spectral observation of C_3 was not until around 100 years after its initial identification in 1881[1] and was realized by detecting the anti-symmetric stretching mode (ν_3) at 2040 cm^{-1} in the circumstellar shell of IRC+10216.[6] Almost simultaneously, the ν_3 fundamental vibration was measured in the laboratory,[21] confirming the astronomical assignment. Further laboratory studies have since measured the ν_1 (symmetric stretching)[22] and ν_2[13] fundamental vibrations. Consequently, it became possible to identify C_3 in space also through its ν_2 mode.[10] Recently, Breier *et al.*[23] extended the ν_2 spectrum of the main C_3 species with spectra of all possible ^{13}C isotopologues using a terahertz-supersonic jet spectrometer in combination with a laser ablation source. In 2013, Krieg *et al.*[24] measured the $\nu_1 + \nu_3$ combination band in high resolution using a home-built continuous-wave optical parametric oscillator (cw-OPO), for the first time probing the 3 μm region of gas-phase C_3. This region is extended in the present study with a large number of new combination bands.

Earlier *ab initio* studies and experimental analysis suggested that the potential energy surface (PES) of C_3 might show a small barrier to linearity.[25] Even more, Matsumura *et al.*[21] concluded from an analysis of the ν_3 fundamental spectrum that this barrier increases when the anti-symmetric stretching vibration is excited. This was based on the observation that the rotational parameter B_v *increases* relative to the ground state parameter when the anti-symmetric stretching vibration is excited. However, the experimental work by Northrup, Sears, and Rohlfing[26] and the theoretical studies by Jensen, Rohlfing, and Almlöf[14] and Mladenović, Schmatz, and Botschwina[15] conclusively showed that C_3 has a linear equilibrium structure. Both theoretical studies clearly showed the strong coupling between the stretching and the bending

a)Electronic mail: doney@strw.leidenuniv.nl

vibrational motions in C_3. Because of this unusual PES, perturbational methods employing an accurate PES were not able to reproduce experimental spectroscopic parameters with the same level of accuracy as seen for other molecules. However, Schröder and Sebald[18] recently developed a high level *ab initio* PES that, when employed in variational ro-vibrational calculations, was able to accurately reproduce experimental spectroscopic parameters for C_3, including those concluded for the $\nu_1 + \nu_3$ band.

Clearly the ro-vibrational spectrum of C_3 is dominated by anharmonic effects. As such, a complete understanding of the PES requires that highly excited vibrational states, particularly those involving multiple vibrational modes, need to be studied. This requires high resolution IR measurements.

In experimental measurements, C_3 molecules are commonly formed either through (1) photolysis of diacetylene, allene, or furan,[21,22,27,28] (2) laser ablation of a carbon rod,[13,24] or (3) a discharge through acetylene.[29,30] To date, these methods have allowed measurements of vibrational states in the electronic ground state (v_1, v_2^{ℓ}, v_3) up to $v_2 = 34$, $v_1 = 3$, and $v_3 = 1$ with v_1, v_2, and v_3 representing the vibrational quantum numbers for the symmetric stretching, the bending, and the antisymmetric stretching vibration, respectively, and ℓ representing the vibrational angular momentum quantum number.

In this paper, we present the experimental spectrum of fifteen bands of gas-phase C_3 in the 3 μm region, including states involving excitation up to $v_1 = 7$ and $v_3 = 3$, and reaching energies of about 11 000 cm^{-1} above the vibrational ground state. This is the first time that these modes have been measured to such high vibrational excitation. We also present new and supporting theoretical ro-vibrational calculations for C_3 that focus on pure stretching states. In Sec. II, we describe the experimental and theoretical approaches. The experimental spectra are presented as collections of band series in Sec. III. A comparison with theoretical results is given in Sec. IV. We summarize with a short conclusion.

II. METHODS

A. Experimental

The experimental setup has been described in detail in Ref. 31, and a similar setup working in the optical has been used to study the $\tilde{A}^1\Pi_u \leftarrow \tilde{X}^1\Sigma_g^+$ $(0, 0^0, 0)$–$(0, 0^0, 0)$ band.[11,30] In the present experiment, a commercial cw-OPO (the Aculight, Argos 2400-SF-B module) that covers ~3110–4200 cm^{-1} is used. This system has been used recently to record high resolution infrared spectra of molecular transients like c-$C_3H_3^+$[32] and HC_6H.[33]

The vibrationally excited C_3 molecules are generated in a pulsed supersonically expanding planar plasma[34] using a precursor gas mixture of 0.5% propyne in 1:1 helium:argon mixture with a 5 bar backing pressure. The gas is expanded into the vacuum chamber through a long thin (0.3 × 30 mm) slit discharge nozzle with an applied high voltage of ~−550 V at the exit. The gas is pulsed using a pulsed valve (General valve, serial 9) connected to the entrance of the nozzle body, with each pulse lasting for about 800 μs. In the past, it was shown that such plasma sources are useful to study vibrationally highly excited species without losing much of the rotational cooling properties in the expansion typical for this type of adiabatic expansions.[35,36]

The high resolution infrared spectrum of the plasma products is recorded using continuous wave cavity ring-down spectroscopy (cw-CRDS), with the IR laser path intersecting the expansion roughly 1 cm downstream from the nozzle body. The optical cavity comprises two plano-concave mirrors with a reflectivity of ~99.98%, centered at 3 μm. Typical empty cavity ring-down times (τ_0) are about 7–9 μs. The hardware (boxcar integrator) based multi-trigger and timing scheme described in detail in Ref. 31 is used to coincide the ring-down event and gas pulse.

The resulting spectrum is recorded in a series of ~1.2 cm^{-1} parts that partially overlap to guarantee that spectra can be directly compared. In total, some 170 cm^{-1} are covered. The Doppler width of the recorded transitions is about 0.004 cm^{-1}. At the same time, the spectrum is recorded and the laser frequency is measured using a wavemeter (Bristol Instruments, 621A-IR), with a resulting maximum frequency uncertainty of ±0.002 cm^{-1}. The frequency accuracy is independently checked by comparing the recorded absorption lines of trace water in the chamber against the corresponding HITRAN values,[37] and typical frequency accuracies of the recorded transitions are better than 0.001 cm^{-1}.

B. Theoretical

The theoretical calculations are based on the recent high-level *ab initio* local PES by Schröder and Sebald[18] for the C_3 molecule ($\tilde{X}^1\Sigma_g^+$). Briefly, the PES is constructed by combining explicitly correlated coupled-cluster results with smaller corrections for core-valence correlation and scalar relativistic and higher-order correlation effects (up to pentuple excitations in coupled-cluster theory). Details on the construction of the PES can be found in the original publication.[18] Due to the excellent performance of the PES in predicting low lying ro-vibrational states,[18] no attempt has been made to adjust the parameters of the PES to the available experimental results. Therefore, the present study provided an excellent test for the reliability of the *ab initio* PES by Schröder and Sebald[18] in predicting highly excited ro-vibrational states in ground state C_3.

The variational ro-vibrational calculations were performed with the RVIB3 program by Carter and Handy[38] and C8VPRO written by Sebald.[39] In order to provide the same level of convergence for higher lying excited ro-vibrational states, the basis set in the RVIB3 calculations is increased compared to the previous calculations.[18] The primitive basis set for the stretching vibrations comprised 200 symmetrized basis functions constructed from 20 functions for both the symmetric and anti-symmetric stretching vibration. For the bending motion, 42 basis functions per $\ell = J, J - 1$, to 0 or 1 are employed. Combining 47 contractions for stretching vibrations per symmetry species with 33 contracted functions for the bending vibration leads to Hamiltonian matrices of dimension 1551 for every value of ℓ. The size of the final Hamiltonian matrix for each symmetry

species is adjusted appropriately in order to provide converged results.

The term energies of ro-vibrational levels for linear molecules can be expressed by

$$T_v(J) = G_v + B_v[J(J+1) - \ell^2] - D_v[J(J+1) - \ell^2]^2, \quad (1)$$

where G_v is the vibrational term energy, B_v the rotational parameter, and D_v is the quartic centrifugal distortion parameter. In Eq. (1), v is a collective variable designating a vibrational state (v_1, v_2^ℓ, v_3) and J is the rotational quantum number. Since all bands observed in this work are Σ–Σ bands, ℓ is equal to 0. Higher-order terms in the expansion of $T_v(J)$ [Eq. (1)] have been neglected due to the strong dependence of such terms on employed J values. This dependence has previously been shown by Schröder and Sebald[18] and will be addressed in more detail in Sec. IV. The transition frequencies between ro-vibrational states v', J' (upper state) and v'', J'' (lower state) is in this case

$$\begin{aligned}\nu = T_{v'}(J') - T_{v''}(J'') = \nu_0 + (B_{v'} + B_{v''})m \\ + [(B_{v'} - B_{v''}) - (D_{v'} - D_{v''})]m^2 \\ - 2(D_{v'} + D_{v''})m^3 - (D_{v'} - D_{v''})m^4, \quad (2)\end{aligned}$$

where $\nu_0 = G_{v'} - G_{v''}$ is the vibrational band origin (VBO), $m = -J''$ for P-branch transitions and $m = J'' + 1$ for R-branch transitions.

While experimentally determined transition frequencies can only be fitted according to Eq. (2), the variationally calculated term energies of an individual vibrational state can also be fitted according to Eq. (1). The results of the latter procedure are termed Calc. I where ro-vibrational states up to $J_{max} = 20$ were employed. Fits of the variationally calculated transition energies according to Eq. (2) employing the same transitions as in the experimental fits are termed Calc. II.

III. RESULTS

The high resolution C_3 plasma spectrum is recorded between 3110 and 3341 cm^{-1}. Additional lines are observed which are due to other propyne plasma products as well as C_3H_4 precursor material. Fifteen bands are observed between 3110–3280 cm^{-1}, with a rotational spacing of ~1.6 cm^{-1}, which is consistent with a 1:0 intensity alternation of ro-vibrational transitions originating from stretching vibrations of C_3; no ro-vibrational bands are observed that can be assigned to transitions involving the bending states. An overview of the C_3 spectra is given in Fig. 1; the observed intensities cannot be directly compared, as these depend, for example, on small variations in the experimental plasma conditions, but general trends can be seen. For example, the C_3 band intensities decrease quickly with decreasing frequency. Assuming a Boltzmann population distribution, this suggests that the lower frequency bands involve transitions starting from higher quanta vibrational states relative to bands at higher frequencies.

The effective experimental band origin and rotational parameters for the lower and upper state of each band are determined using the spectral fitting software Pgopher.[40] Preliminary spectral analysis of the fifteen bands is performed by fitting the observed transitions to simulated spectra assuming $B_v \sim 0.4\ cm^{-1}$ and using transition intensities near the band origins to determine the state symmetry (either Σ_g^+ or Σ_u^+). For most of the bands, transitions could be assigned up to $J'' = 20$ (see the supplementary material). From the rotational profiles, the rotational temperature of C_3 is determined to be about 55 K. This is slightly higher than typical for the plasma source in use.[33,41] A least-squares fit analysis based on Eq. (2) is then used to determine tentative vibrational band origins (VBOs) and lower and upper rotational parameters, $B_{v''}$ and $B_{v'}$, respectively. The bands are labeled A–O in descending value of their VBO.

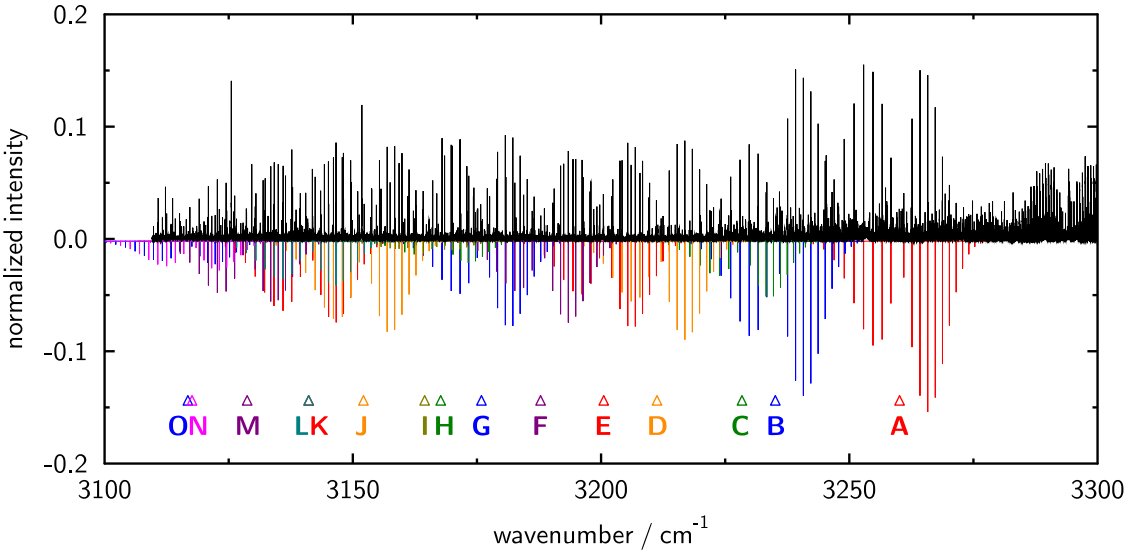

FIG. 1. The experimental (in black) spectrum of the propyne plasma products showing a series of bands, which are assigned to vibrationally excited C_3 (simulated bands from Pgopher, inverted). The strong bands at frequencies higher than 3275 cm^{-1} are assigned to propyne. The bands are assigned to the transitions: (A) (1, 0^0, 1)–(0, 0^0, 0), (B) (2, 0^0, 1)–(1, 0^0, 0), (C) (1, 0^0, 2)–(0, 0^0, 1), (D) (3, 0^0, 1)–(2, 0^0, 0), (E) (2, 0^0, 2)–(1, 0^0, 1), (F) (4, 0^0, 1)–(3, 0^0, 0), (G) (3, 0^0, 2)–(2, 0^0, 1), (H) (2, 0^0, 3)–(1, 0^0, 2), (I) (5, 0^0, 1)–(4, 0^0, 0), (J) (4, 0^0, 2)–(3, 0^0, 1), (K) (3, 0^0, 3)–(2, 0^0, 2), (L) (6, 0^0, 1)–(5, 0^0, 0), (M) (5, 0^0, 2)–(4, 0^0, 1), (N) (7, 0^0, 1)–(6, 0^0, 0), and (O) (4, 0^0, 3)–(3, 0^0, 2).

Initial fits of the bands showed that some of them share vibrational states, i.e., the determined $B_{v'}$ for one band is the same as the $B_{v''}$ for another band. Based on the rotational parameters and state symmetry, twelve of the bands can be grouped into five vibrational series involving common states: A–E–K; B–G–O; C–H; D–J; and F–M. The other bands do not share common states. VBOs of each band in a series, regardless of the series, are separated by about 60 cm^{-1}, suggesting that in all five series, the lower state of each band is increasing by the same number of quanta, which based on frequency region, is likely $\Delta v_1 = 1$ and $\Delta v_3 = 1$. This is also clearly visible from Fig. 1. In addition, seven of the bands, A, B, D, F, I, L, and N, are evenly separated by about 23 cm^{-1}, suggesting that they are also part of a different progression that increases by $\Delta v_1 = 1$ in the lower state.

In order to confirm the initial assignment, the experimental line positions, determined by the PGOPHER software,[40] are compared to the results of the variational calculations. Figure 2 depicts the difference between experimental and variationally calculated line positions, $\Delta\nu$. These line positions are available in the supplementary material. For all bands, the differences are smaller than 1 cm^{-1}, except for band N which has a difference of 1.5 cm^{-1}. This agreement confirms the vibrational assignment of the observed bands. Additionally, the lower panel of Fig. 2 shows the differences when the error in the VBOs is subtracted, $\Delta\nu$–$\Delta\nu_0$. The errors are decreased by more than an order of magnitude, unambiguously confirming the rotational assignment of the individual lines within the bands. For two of the observed bands, bands L and M, deviations from the expected independence of the errors from the rotational quantum number are observed. This indicates a local anharmonic resonance, which will be discussed in detail below.

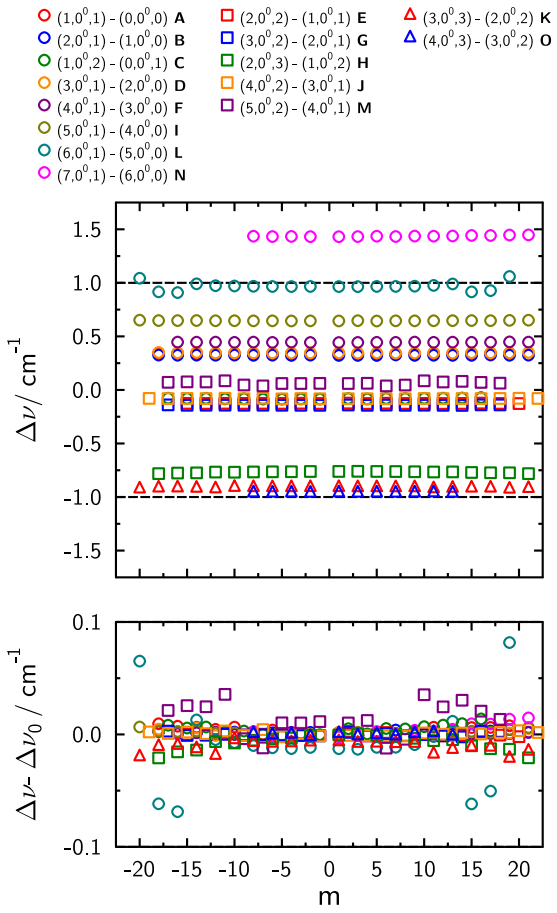

FIG. 2. Comparison of experimental and variationally calculated line positions, $\Delta\nu$, for the fifteen observed combination bands of C_3 showing the accuracy in predicting the vibrational energy. The J dependent accuracy is highlighted in the plot of $\Delta\nu$–$\Delta\nu_0$. Identical colors refer to bands in one series with the circle, square, and triangle markers referring to the first, second, and third band in the series, respectively. The larger deviations seen for bands L and M are due to a difference in the determined location of state crossings, as discussed in the text.

TABLE I. Band origins (in cm^{-1}) and assignments (v_1, v_2^{ℓ}, v_3) of the observed C_3 combination bands.

		ν_0	
Label	Assignment	Expt.[a]	Calc. II
A	(1, 0^0, 1)–(0, 0^0, 0)	3260.1265(4)	3259.79
B	(2, 0^0, 1)–(1, 0^0, 0)	3235.0964(4)	3234.77
C	(1, 0^0, 2)–(0, 0^0, 1)	3228.3796(4)	3228.46
D	(3, 0^0, 1)–(2, 0^0, 0)	3211.2653(4)	3210.92
E	(2, 0^0, 2)–(1, 0^0, 1)	3200.5361(4)	3200.66
F	(4, 0^0, 1)–(3, 0^0, 0)	3187.8158(4)	3187.37
G	(3, 0^0, 2)–(2, 0^0, 1)	3175.9066(4)	3176.05
H	(2, 0^0, 3)–(1, 0^0, 2)	3167.7016(4)	3168.46
I	(5, 0^0, 1)–(4, 0^0, 0)	3164.4665(4)	3163.82
J	(4, 0^0, 2)–(3, 0^0, 1)	3152.1415(4)	3152.22
K	(3, 0^0, 3)–(2, 0^0, 2)	3141.1229(4)	3142.03
L	(6, 0^0, 1)–(5, 0^0, 0)	3141.0896(4)	3140.11
M	(5, 0^0, 2)–(4, 0^0, 1)	3128.7178(4)	3128.66
N	(7, 0^0, 1)–(6, 0^0, 0)	3117.6110(5)	3116.18
O	(4, 0^0, 3)–(3, 0^0, 2)	3116.7759(5)	3117.74

[a]Experimental uncertainties are given in parentheses in units of the last significant digits.

Systematic rotational analysis of the observed bands is carried out by fitting the experimental transitions with linked states simultaneously according to Eq. (2). The resultant experimental VBOs of the fifteen bands are given in Table I together with the corresponding variational results (Calc. II). The experimental and theoretical (Calc. I and Calc. II) rotational parameters are summarized in Table II. Typically the results of the latter two fits are observed to deviate by less than 1% in the quartic centrifugal distortion parameter.

A. The (3, 0^0, 3)–(2, 0^0, 2)–(1, 0^0, 1)–(0, 0^0, 0) band series

The strongest transitions in the experimental spectrum associated with C_3 (band A, Fig. 3), belong to the known combination band (1, 0^0, 1)–(0, 0^0, 0) with a band origin at 3260.13 cm^{-1}.[24] The combination band is of symmetry type Σ_u^+–Σ_g^+ and exhibits the characteristic intensity alternation of 1:0 for even and odd J-levels due to the nuclear spin statistical weights for equivalent carbon atoms. The ground state rotational parameter is determined to be 0.430 569(3) cm^{-1}, which is in agreement with the literature values,[13,24,27,29] and the quartic centrifugal distortion parameter, D_v, is 1.399(12) $\times 10^{-6}$ cm^{-1}, smaller by about 5% compared to the value by Krieg *et al.*[24] of 1.471(13) $\times 10^{-6}$ cm^{-1}. Similarly, the VBO, which in this case is equal to G_v, and the (1, 0^0, 1) state rotational parameter are determined to be 3260.1265(4) and

TABLE II. Effective experimental and theoretical spectroscopic parameters of C_3 (in cm^{-1}).

	B_v			$10^6\ D_v$		
State	Expt.[a]	Calc. I	Calc. II	Expt.[a]	Calc. I	Calc. II
(0, 0^0, 0)	0.430569(3)	0.430 61	0.430 62	1.399(12)	1.437	1.450
(1, 0^0, 1)	0.424211(8)	0.424 23	0.424 23	1.110(27)	1.143	1.144
(2, 0^0, 2)	0.418208(9)	0.418 24	0.418 23	0.894(21)	0.946	0.936
(3, 0^0, 3)	0.412448(8)	0.412 52	0.412 51	0.737(18)	0.812	0.806
(1, 0^0, 0)	0.424997(5)	0.425 01	0.425 01	0.704(16)	0.693	0.708
(2, 0^0, 1)	0.419489(5)	0.419 50	0.419 50	0.610(14)	0.613	0.614
(3, 0^0, 2)	0.414065(8)	0.414 10	0.414 12	0.530(28)	0.550	0.607
(4, 0^0, 3)	0.408807(14)	0.408 80	0.408 80	0.565(48)	0.499	0.520
(0, 0^0, 1)	0.435664(8)	0.435 54	0.435 56	3.890(10)	3.763	3.825
(1, 0^0, 2)	0.427040(6)	0.426 90	0.426 90	2.749(17)	2.691	2.696
(2, 0^0, 3)	0.419519(7)	0.419 43	0.416 43	2.035(17)	1.998	1.987
(2, 0^0, 0)	0.421603(6)	0.421 64	0.421 64	0.441(14)	0.462	0.461
(3, 0^0, 1)	0.416385(4)	0.416 41	0.416 42	0.416(9)	0.438	0.439
(4, 0^0, 2)	0.411212(6)	0.411 23	0.411 24	0.392(14)	0.406	0.410
(3, 0^0, 0)	0.419074(8)	0.419 07	0.419 08	0.467(21)	0.372	0.395
(4, 0^0, 1)	0.413969(6)	0.413 95	0.413 96	0.439(14)	0.355	0.372
(5, 0^0, 2)	0.408958(11)	0.408 70	0.408 76	0.529(33)	–0.195	0.023
(4, 0^0, 0)	0.416862(6)	0.416 86	0.416 87	0.345(14)	0.324	0.328
(5, 0^0, 1)	0.411807(6)	0.411 80	0.411 80	0.310(12)	0.314	0.314
(5, 0^0, 0)	0.414818(55)	0.414 86	0.414 87		0.292	0.316
(6, 0^0, 1)	0.409740(51)	0.410 10	0.410 27		1.056	1.797
(6, 0^0, 0)	0.412989(9)	0.412 98	0.412 99	0.743(24)	0.276	0.577
(7, 0^0, 1)	0.408009(8)	0.407 95	0.407 97	0.699(20)	0.276	0.540

[a]Experimental uncertainties are given in parentheses in units of the last significant digits.

0.424 211(8) cm^{-1}, respectively, in agreement with the values determined by Krieg *et al.*[24] 3260.127 048(91) and 0.424 199 0(25) cm^{-1}, respectively. D_v for the (1, 0^0, 1) agrees to within 3% with the value of Krieg *et al.*[24] The observed line positions (see the supplementary material) agree with those observed by Krieg *et al.*[24] Moreover, both the ground and (1, 0^0, 1) state VBO and B_v agree to within 0.01% with the theoretical values (Tables I and II). We note that in both our spectrum and that of Krieg *et al.*,[24] the best fit observed-calculated (o-c) values suggest a small perturbation around $J' = 9$. This slight anharmonic interaction in the (1, 0^0, 1) state is successfully predicted by the present variational calculation, which is seen by no noticeable deviation in the $\Delta\nu$–$\Delta\nu_0$ plot in Fig. 2. An analysis of the term energies and state orderings showed that the most likely state responsible is the (1, 19^1, 0) state, which crosses the (1, 0^0, 1) state between $J = 8$ and 9. Further anharmonic resonances have been predicted by Schröder and Sebald[18] to occur with states of the (2, 7^ℓ, 0) manifold for $J' \geq 19$.

Simultaneous fitting of bands A, E, and K (Fig. 3) gives VBOs for bands E and K of 3200.5361(4) and 3141.1229(4) cm^{-1}, which translate into upper state vibrational term energies of 6460.6640(3) and 9601.7887(5) cm^{-1}, respectively. As close multiples of the energy for (1, 0^0, 1), bands E and K are assigned the (2, 0^0, 2)–(1, 0^0, 1) (Σ_g^+–Σ_u^+) and (3, 0^0, 3)–(2, 0^0, 2) (Σ_u^+–Σ_g^+) combination bands, respectively. The assignment is confirmed by comparing the experimental rotational parameters for the (2, 0^0, 2) and the (3, 0^0, 3) states to the corresponding values obtained variationally. The B_v values are in almost perfect agreement, with differences of less than 0.002%. Likewise, agreement of experimental and theoretical quartic centrifugal distortion, D_v, parameters is good except for the (3, 0^0, 3) which might indicate a perturbation.

B. The (4, 0^0, 3)–(3, 0^0, 2)–(2, 0^0, 1)–(1, 0^0, 0) band series

Based on the VBO, rotational parameter, and state symmetry (Σ_g^+) determined from the least-squares fitting, the lower state of the second strongest band (band B) is assigned to (1, 0^0, 0). The rotational parameter, B_v, is determined to be 0.424 997(5) cm^{-1} and agrees with the value of 0.424 950(62) cm^{-1} determined for the ν_1 fundamental from the electronic spectra by Zhang *et al.*[22] as well as the current calculations (0.425 01 cm^{-1}). A value of 0.704(16) × 10^{-6} cm^{-1} is obtained for the (1, 0^0, 0) state D_v. This value is within the somewhat larger error bars of D_v determined from the electronic spectra[22] of 0.52(23) × 10^{-6} cm^{-1}.

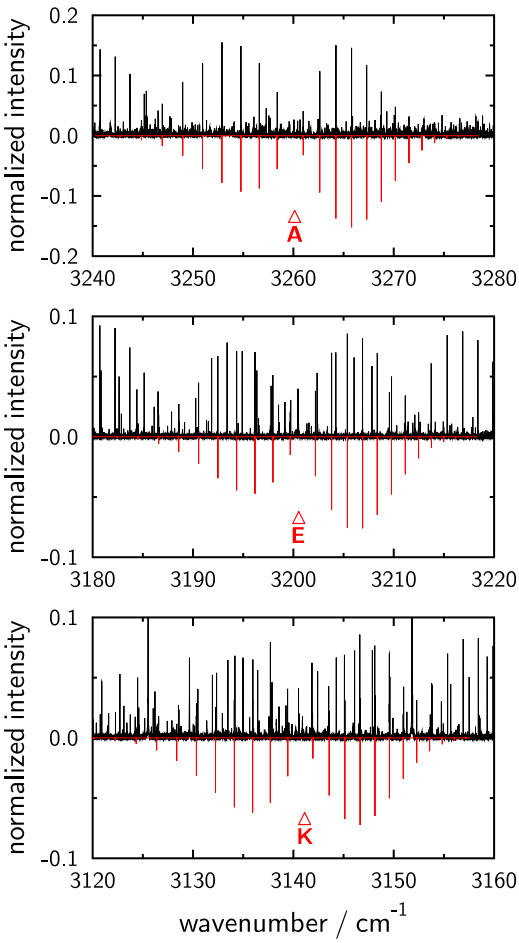

FIG. 3. The experimental (in black) and simulated (from PGOPHER, inverted) spectra of the C_3 bands: (A) (1, 0^0, 1)–(0, 0^0, 0), (E) (2, 0^0, 2)–(1, 0^0, 1), and (K) (3, 0^0, 3)–(2, 0^0, 2).

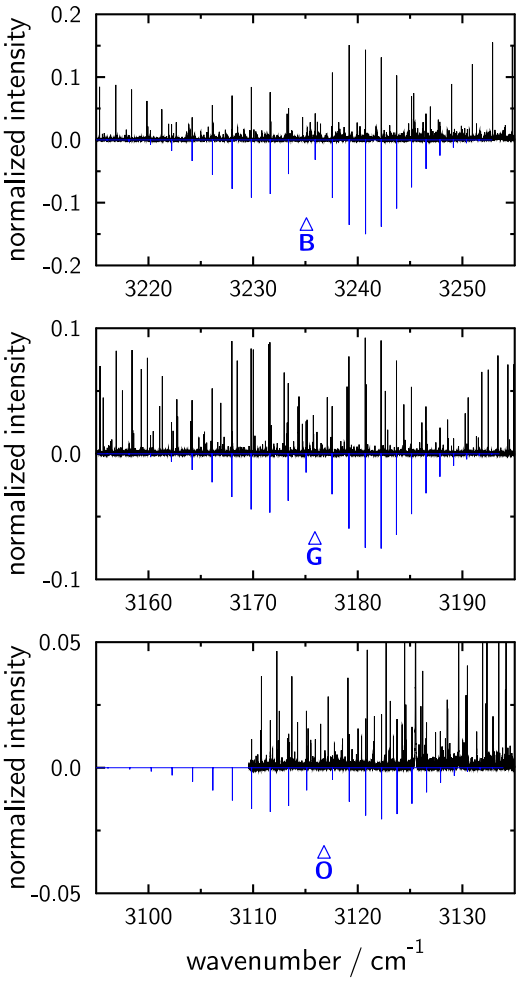

FIG. 4. The experimental (in black) and simulated (from PGOPHER, inverted) spectra of the C_3 bands: (B) (2, 0^0, 1)–(1, 0^0, 0), (G) (3, 0^0, 2)–(2, 0^0, 1), and (O) (4, 0^0, 3)–(3, 0^0, 2).

Assuming an increase of $\Delta v_1 = 1$ and $\Delta v_3 = 1$ in the quantum numbers, the bands in this series, B, G, and O (Fig. 4), are assigned to the (2, 0^0, 1)–(1, 0^0, 0) (Σ_u^+–Σ_g^+), (3, 0^0, 2)–(2, 0^0, 1) (Σ_g^+–Σ_u^+), and (4, 0^0, 3)–(3, 0^0, 2) (Σ_u^+–Σ_g^+) combination bands, respectively. Simultaneous fitting of bands B, G, and O gives VBOs consistent with those expected for all three bands (Table I). Furthermore, the experimentally determined and variationally calculated rotational parameters B_v agree to within 0.002%. However, for the (4, 0^0, 3) level, both theoretical fits (Calc. I and Calc. II) predict a D_v value smaller than that for (3, 0^0, 2), which is not observed experimentally. This discrepancy is caused by the fact that band O is only observed up to P(8). While the spectroscopic parameters of the (3, 0^0, 2) are constrained by transitions in band G, (4, 0^0, 3) has no such additional information, and the limited observed transitions for band O severely skews the experimental fit, resulting in a large uncertainty in the determined D_v value. This effect can also be observed by comparing the D_v obtained from Calc. I and Calc. II. By employing the same lines as observed experimentally and fitting bands B, G, and O simultaneously (Calc. II), D_v of (4, 0^0, 3) increases by about 4% compared to the Calc. I result. A similar but less pronounced effect is also observed for the D_v of (1, 0^0, 0), where the Calc. II result is larger than the Calc. I result almost coinciding with the experimental value;

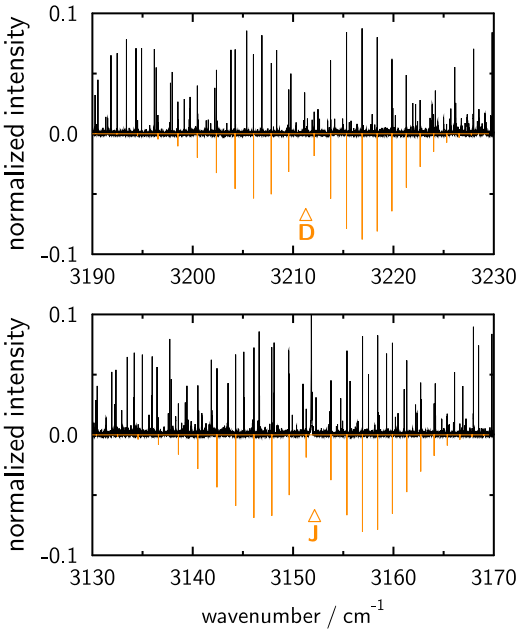

FIG. 5. The experimental (in black) and simulated (from PGOPHER, inverted) spectra of the C_3 bands: (D) (3, 0^0, 1)–(2, 0^0, 0) and (J) (4, 0^0, 2)–(3, 0^0, 1).

see Table II. As such, the theoretical values (Calc. I) are likely closer to the true value for the (4, 0^0, 3) state.

C. The (4, 0^0, 2)–(3, 0^0, 1)–(2, 0^0, 0) band series

Band D starts this series (Fig. 5) and is the third band in the large progression. From the least-squares fit analysis, the VBO is determined to be 3211.2653(4) cm^{-1}, which agrees to within about 0.3 cm^{-1} with the variational result for the (3, 0^0, 1)–(2, 0^0, 0) band (Table I). Therefore, band D is assigned to the (3, 0^0, 1)–(2, 0^0, 0) (Σ_u^+–Σ_g^+) combination band, thereby confirming that the larger progression is a progression of (v_1, 0^0, 0) where the lower state of each band increases by $\Delta v_1 = 1$. This assignment is further confirmed by the agreement of the experimental and theoretical rotational parameters (Table II).

Simultaneous fitting of transitions in band D and band J confirm that they share a common energy level, (3, 0^0, 1). Consequently, band J is assigned to the (4, 0^0, 2)–(3, 0^0, 1) (Σ_g^+–Σ_u^+) combination band. The experimental VBO is 3152.1415(4) cm^{-1} only 0.08 cm^{-1} lower than the value calculated variationally. For both bands D and J, the experimental and calculated rotational B_v parameters differ by no more than 0.01% (Table II).

D. The (5, 0^0, 2)–(4, 0^0, 1)–(3, 0^0, 0) band series

As with the last series, this series is assumed to start with the lower state of the first band being a vibrationally excited state of type (v_1, 0^0, 0). Based on the comparison of experimental and theoretical VBO and rotational parameters (Tables I and II), band F is assigned to the (4, 0^0, 1)–(3, 0^0, 0) (Σ_u^+–Σ_g^+) combination band. Simultaneous fitting of bands F and M (Fig. 6) confirms that they share an energy level, (4, 0^0, 1), and band M is assigned to the (5, 0^0, 2)–(4, 0^0, 1) (Σ_g^+–Σ_u^+) combination band.

Band M shows signs of a small local anharmonic resonance likely within the (5, 0^0, 2) state, which can be further deduced from the larger deviations in the D_v parameter for the (5, 0^0, 2) state. Based on the o-c value of the experimental line positions (see the supplementary material), a perturbation occurs around $J = 3$. According to the variational calculations, the (5, 0^0, 2) state is expected to be crossed by the (4, 10^2, 2) state between $J = 6$ and 7 and by the (4, 10^0, 2) state between $J = 8$ and 9. The mismatch in the position of the crossing results in the observed down-up-down deviation seen in the $\Delta\nu$–$\Delta\nu_0$ plot in Fig. 2. The state density near 9900 cm^{-1} is extremely high; there are about 6 states for $J = 6$ and 8 states for $J = 8$ within ±10 cm^{-1} of the (5, 0^0, 2) state. Therefore, the influence of other nearby states might be non-negligible. However, inspection of expansion coefficients of the ro-vibrational wavefunction makes the two (4, 10^ℓ, 2) states the most likely ones that cause the local anharmonic resonances.

E. The (5, 0^0, 1)–(4, 0^0, 0), (6, 0^0, 1)–(5, 0^0, 0), and (7, 0^0, 1)–(6, 0^0, 0) bands

The bands I, L, and N (Fig. 7) do not share a state with any other observed band, but they are part of the larger

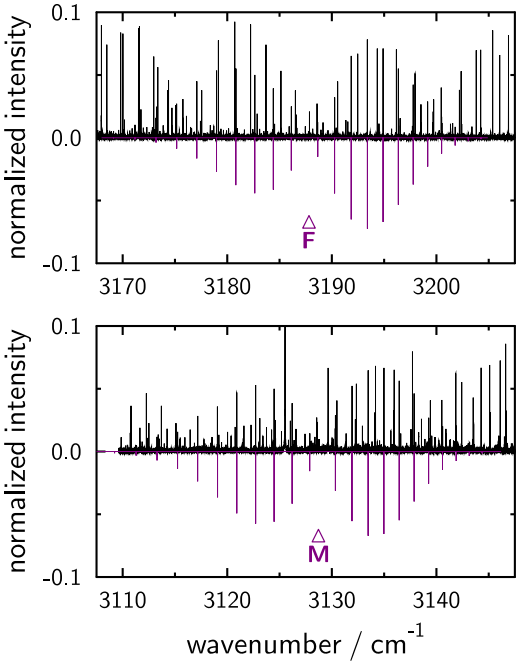

FIG. 6. The experimental (in black) and simulated (from Pgopher, inverted) spectra of the C_3 bands: (F) (4, 0^0, 1)–(3, 0^0, 0) and (M) (5, 0^0, 2)–(4, 0^0, 1).

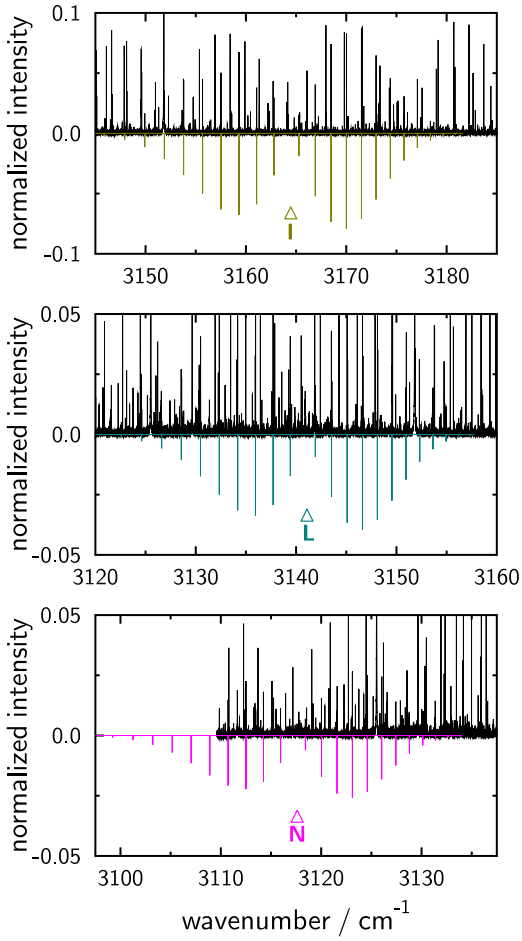

FIG. 7. The experimental (in black) and simulated (from Pgopher, inverted) spectra of the C_3 bands: (I) (5, 0^0, 1)–(4, 0^0, 0), (L) (6, 0^0, 1)–(5, 0^0, 0), and (N) (7, 0^0, 1)–(6, 0^0, 0).

$(v_1, 0^0, 0)$ progression. Based on their VBOs and relative intensities in the progression, the three bands are assigned to the (5, 0^0, 1)–(4, 0^0, 0) (Σ_u^+–Σ_g^+), (6, 0^0, 1)–(5, 0^0, 0) (Σ_g^+–Σ_u^+), and (7, 0^0, 1)–(6, 0^0, 0) (Σ_u^+–Σ_g^+) bands, respectively. The experimental VBOs of 3164.4665(4), 3141.0896(4), and 3117.6110(5) for bands I, L, and N, respectively, agree to within 0.65, 0.98, and 1.43 cm^{-1} with the predicted VBOs (Table I). The experimental B_v values for each band show differences of 0.0004% to 0.09% compared to the values obtained in the variational calculations, confirming the assignment. As seen with band O, the disagreement between the experimental and theoretical D_v values for band N is a result of the limited observation of P-branch transitions.

Unlike any of the other observed bands, band L is heavily perturbed, with a strong perturbation in the form of an avoided crossing seen in the o-c values at $J' = 13$ and 15. In fact, for the $J' = 15$ transitions, the best fit o-c values are about -0.04 cm^{-1}, almost two orders of magnitude larger than the average residuals for all other C_3 transitions. Because the perturbation occurs at a higher J'', no D_v parameter can reliably be determined from our experimental fit. Indeed, an avoided crossing is predicted by the variational calculations for the (6, 0^0, 1) state. The perturbing (4, 3^1, 2) state lies at a frequency lower than the (6, 0^0, 1) state for $J \leq 18$ and crosses to a higher frequency between $J = 18$ and 19. As discussed for the (5, 0^0, 2) state, the down-up deviation seen in the $\Delta\nu$–$\Delta\nu_0$ plot in Fig. 2 for band L is due to a disagreement in the position of the crossing. Furthermore, the interaction between the (6, 0^0, 1) and (4, 3^1, 2) states is much stronger than that predicted for the (5, 0^0, 2) state, which is seen in the larger magnitude of the deviations in the $\Delta\nu$–$\Delta\nu_0$ plot in Fig. 2 and in the larger experimental o-c values.

F. The (2, 0^0, 3)–(1, 0^0, 2)–(0, 0^0, 1) band series

The last of the vibrational series, comprising bands C and H (Fig. 8), is unconnected to the other series. Based on the least-squares fit of band C, the lower state (Σ_u^+ symmetry) is assigned to (0, 0^0, 1). The rotational parameter, B_v, is determined to be 0.435 664(8) cm^{-1} to be compared with the value of 0.435 696 9(56) cm^{-1} obtained by Krieg *et al.*[24] For the quartic centrifugal distortion parameter D_v, a value of 3.890(10) $\times$ 10^{-6} cm^{-1} is obtained, which is lower by 11% compared to the value of Krieg *et al.*[24] These discrepancies can be explained by the different truncations of the $J(J + 1)$ expansion of the rotational energy employed in this study (up to D_v) and by Krieg *et al.*[24] (up to M_v) as well as different J levels observed in both experiments. However, the strong increase in D_v by factor of about 3 compared to the vibrational ground state is consistent with an excited state of the anti-symmetric stretching vibration. Therefore, band C is assigned the (1, 0^0, 2)–(0, 0^0, 1) (Σ_g^+–Σ_u^+) transition. The assignment is also confirmed by comparing experimental and theoretical lower and upper state rotational parameters which agree with 0.03% and 3% for B_v and D_v, respectively.

Simultaneous fitting of bands C and H confirms a shared state, (1, 0^0, 2). As such, band H is assigned to the (2, 0^0, 3)–(1, 0^0, 2) (Σ_u^+–Σ_g^+) combination band. The corresponding VBO of 3167.7016(4) cm^{-1} agrees to within 0.76 cm^{-1} with the Calc. II value (Table I). Both the upper and lower state rotational parameters, B_v, agree with the present *variational results*. In fact, the differences do not exceed 0.03% for the B_v and 2% for the centrifugal distortion parameter D_v.

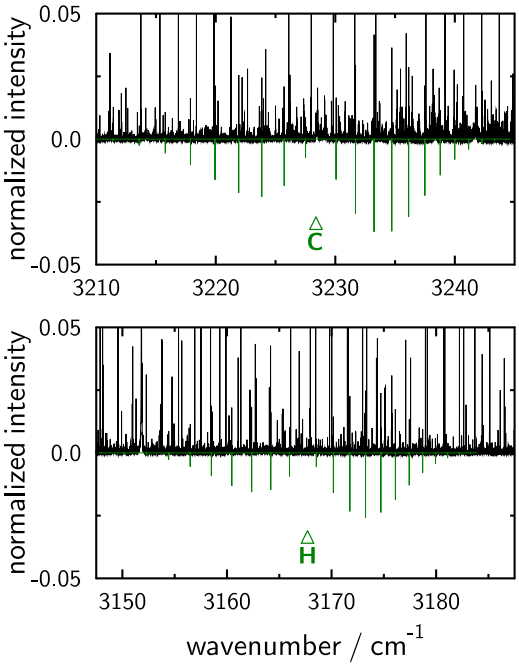

FIG. 8. The experimental (in black) and simulated (from PGOPHER, inverted) spectra of the C_3 bands: (C) (1, 0^0, 2)–(0, 0^0, 1) and (H) (2, 0^0, 3)–(1, 0^0, 2).

IV. DISCUSSION

From the fifteen observed C_3 combination bands, v_1 is observed up to 6 quanta, and v_3 is observed up to 2 quanta, in the respective lower state. This is expected given that v_1 requires less energy to populate. The intensities of the observed bands approximately follow that expected from a Boltzmann distribution, for both the bands that are part of the larger (v_1, 0^0, 0) progression and between bands in the same vibrational series.

Given the excellent agreement between the experimental and theoretical spectroscopic parameters, a closer look at the trends observed for said parameters appears promising. Furthermore, we wish to discuss the results also with respect to a second-order vibrational perturbation theory (VPT2) treatment. Therefore, using finite differences, the PES of Schröder and Sebald[18] was transformed to a quartic force-field (QFF) in normal coordinates and the parameters are given in Table III. The normal coordinate force constants reflect the highly anharmonic nature of the C_3 molecule. For example, the diagonal quartic bending force constant k_{2222} is calculated to be 724.835 cm^{-1}, which is larger by a factor of about 17 compared to the harmonic bending frequency of $\omega_2 = 42.773$ cm^{-1}. The strong coupling between the symmetric stretching and the bending vibration is apparent from the value of the cubic coupling constant $k_{122} = 1315.426$ cm^{-1}, which is even larger than the harmonic frequency of the symmetric stretching vibration ($\omega_1 = 1206.698$ cm^{-1}). These large

TABLE III. Parameters (in cm^{-1}) of the quartic force field in dimensionless normal coordinates for C_3.[a]

Parameter[b]	Value	Parameter[b]	Value
ω_1	1206.698	k_{1111}	1.717
ω_2	42.773	k_{1122}	−177.462
ω_3	2101.276	k_{1133}	17.789
k_{111}	−41.975	k_{2222}	724.835
k_{122}	1315.426	k_{2233}	−294.533
k_{133}	−211.964	k_{3333}	5.131

[a]The equilibrium bond length is R_e = 1.293 97 Å.
[b]The cubic k_{ijk} and quartic k_{ijkl} force field parameters are defined according to the work of Nielsen.[42]

third- and fourth-order force constants clearly show that a perturbational treatment of any order for the vibration-rotation problem in C_3 is problematic.

In Fig. 9, the differences $\Delta B_v = B_v - B_0$ for selected vibrational states of C_3 are depicted, where B_0 corresponds to the rotational parameter B_v of the vibrational ground state. Near perfect agreement of the experimental and theoretical results is observed, except for the perturbed states $(5, 0^0, 2)$ and $(6, 0^0, 1)$. In the case of a well behaved semi-rigid molecule, this difference can be written within VPT2 as $\Delta B_v = -\sum_i \alpha_i \cdot v_i$. Hence, ΔB_v is a linear function of the quantum numbers v_i, and in general one observes only small deviations from linearity for higher values of v_i as a result of higher-order perturbation effects. In C_3, strong deviations from linearity can be observed for *low* values of v_1, while for higher values of v_1, a near linear dependency is found (see left panel of Fig. 9). In fact, a linear fit of the $(v_1, 0, 0)$ series from $v_1 = 3$ to 6 results in an effective α_1 of 0.0020 cm^{-1} for both the experimental and theoretical ΔB_v values. However, employing the standard procedure of determining an effective α_1 as the difference of B_v between the vibrational ground and $(1, 0^0, 0)$ state results in 0.0056 cm^{-1} from experimental and variational results. Finally, α_1 calculated within VPT2 using the present QFF is 0.0014 cm^{-1}. The latter value is closer to the results from the linear range than α_1 calculated from B_v in the $(0, 0^0, 0)$ and $(1, 0^0, 0)$ state. This behavior will be explained below.

In the right panel of Fig. 9, the variation of ΔB_v with v_3 is depicted. Again, a strong nonlinear dependency on v_3 can be seen. Here, even the sign of the slope changes when excitation in v_1 is added. From the experimental and variationally calculated $(4, 0^0, v_3)$ ΔB_v series (v_3 = 0 to 3), an effective α_3 of 0.0027 cm^{-1} is obtained. Again, this value is intermediate between the VPT2 result of $\alpha_3 = 0.0034$ cm^{-1} and the α_3 values of −0.0051 and −0.0050 cm^{-1} (experimental and variational results, respectively) obtained by considering only the $(0, 0^0, 0)$ and $(0, 0^0, 1)$ states. Both findings can be explained by the fact that the bending part of the PES becomes more stiff upon excitation of the symmetric stretching vibration. Starting from certain values of v_1, a linear dependency of B_v with respect to the v_i can be observed, which is characteristic for semi-rigid molecules.

The dependence of B_v on the stretching quantum numbers v_1 and v_3 can be understood by considering the vibrational wavefunctions. In order to quantify the relation between the vibrational wavefunctions and the rotational parameters, we have calculated the integrated density of the vibrational wavefunction as a function of the bond angle according to

$$\bar{P}_v(t) = \int_{q_2=0}^{t} q_2 \mathrm{d}q_2 \int_{q_1=-\infty}^{\infty} \mathrm{d}q_1 \int_{q_3=-\infty}^{\infty} \mathrm{d}q_3 \times \Psi_v^*(q_1, q_3, q_2)\Psi_v(q_1, q_3, q_2). \quad (3)$$

In Eq. (3), Ψ_v is the normalized vibrational wavefunction of the vibrational state under consideration obtained variationally with the C8VPRO program[39] and the q_i are dimensionless normal coordinates. Integration over the complete configuration space of vibrational coordinates yields a value of 1. If one treats the upper limit t of the integration over q_2 as a parameter, it is possible to calculate the dependency of the integrated density on the deviation of the bond angle from linearity, θ. The value of $q_2 = t$ can be connected to θ by

$$\theta = 2 \arctan\left(\frac{q_2(t^x_{12} - t^x_{22})}{R_e}\right). \quad (4)$$

Here, R_e is the equilibrium bond length and t^x_{ij} are appropriate t-matrix elements (the t-matrix connects dimensionless normal coordinates with Cartesian displacement coordinates).

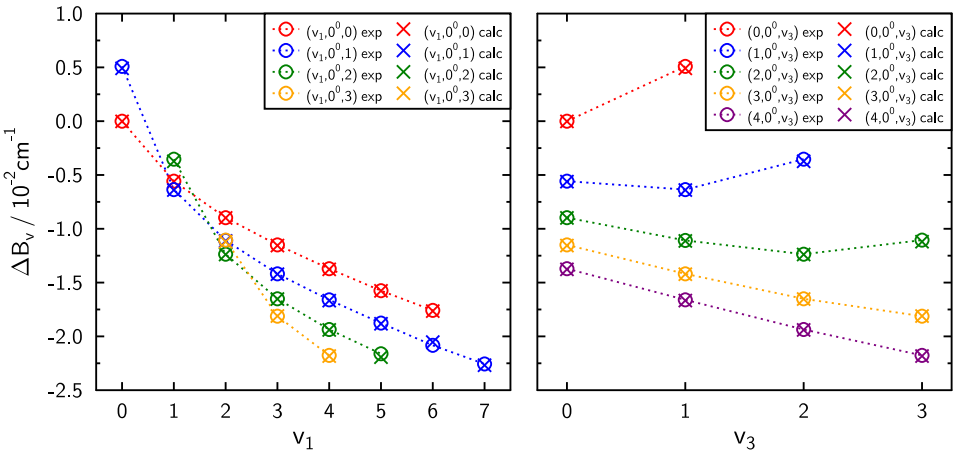

FIG. 9. Left panel: variation of B_v with increasing stretching quantum numbers v_1 for different series of fixed quantum numbers v_3 and right panel: variation of B_v with increasing stretching quantum numbers v_3 for different series of fixed quantum numbers v_1.

Thus, $\bar{P}_v(t)$ gives a qualitative impression of how the probability density accumulates as a function of the bond angle. The larger the angle where $\bar{P}_v(t)$ reaches the region of the asymptotic value of 1, the greater the bent character of the state under consideration. In Fig. 10, $\bar{P}_v(t)$ is depicted for fifteen states investigated experimentally in this work and for a further four states, namely, (0, 1^1, 0), (0, 2^0, 0), (0, 2^0, 2), and (0, 0^0, 2), for a better understanding.

In a well behaved semi-rigid molecule, like CO_2, $\bar{P}_v(t)$ for a stretching vibrational state reaches a value close to the asymptote quite early ($\theta \approx 15°$) and is nearly independent of the combination of stretching vibrational quantum numbers. A value of $\theta > 0$ is always to be expected because of the zero point motion of the molecule. By contrast, in C_3, one finds a strong dependence on the stretching vibrational quantum numbers.

In the upper panel of Fig. 10, the vibrational ground state clearly exhibits the most bent character among the pure symmetric stretching states. In the middle panel, one can observe that the fundamental antisymmetric stretching state (0, 0^0, 1) reaches the asymptotic value as late as the fundamental bending state. Consequently B_v of the (0, 0^0, 1) state is *larger* than the rotational parameter in the vibrational ground state.

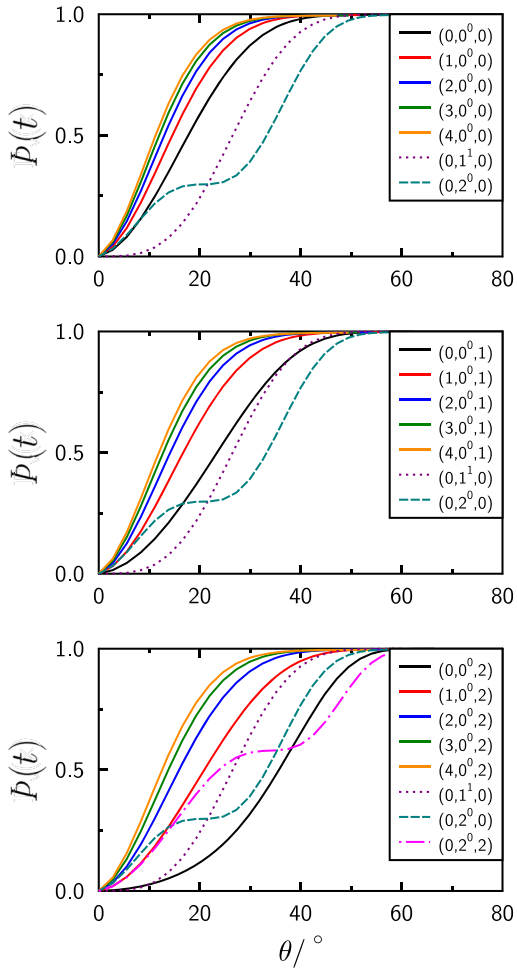

FIG. 10. Integrated densities of vibrational wavefunctions as a function of the deviation from linearity θ for three series of C_3 states: (top) (v_1, 0^0, 0), (middle) (v_1, 0^0, 1), and (bottom) (v_1, 0^0, 2) using the (0, 1^1, 0) and (0, 2^0, 0) states as reference.

Figure 10 also suggests that the state (1, 0^0, 2) collects its density at larger angles than (1, 0^0, 1). Indeed, the state (1, 0^0, 2) is a further example where the rotational parameter B_v becomes larger upon excitation of one quanta in the anti-symmetric stretching vibration. In the lower panel of Fig. 10, it can be seen that the first overtone of the antisymmetric stretching vibration (0, 0^0, 2) accumulates most of its density at even *larger* θ values than the first overtone of the bending vibration (0, 2^0, 0). The lower panel of Fig. 10 also suggests that the (0, 2^0, 2) state accumulates most of its density at smaller angles than the (0, 0^0, 2) state, resulting in a *smaller* rotational parameter. This is really found in our calculations assuming the rotational pattern of a linear molecule in the range $J = 0$ to 10 with B_v of 0.4575 and 0.4565 cm^{-1} for (0, 0^0, 2) and (0, 2^0, 2), respectively.

These observations are in line with the well-known fact that C_3 exhibits more and more the properties of a bent molecule with increasing excitation of the anti-symmetric stretching vibration.[43] Therefore, the rotational pattern of stretching vibrational states which show more or less bent character cannot accurately be described by neither the formulas for a linear molecule [see Eq. (1)] nor those of an asymmetric top molecule. Hence, more or less long progressions in $J(J + 1)$ are necessary to fit the rotational energies with the same accuracy as those states which are not affected by this issue. This has been done in previous experimental work[21,24,27] resulting in slightly different rotational parameters compared to those obtained in the present work. As C_3 has a linear equilibrium structure, it is definitely not a quasilinear molecule. The quasilinearity parameter γ_0 introduced by Yamada and Winnewisser[44] equals to −0.91 which corresponds to an almost linear molecule. Given the growing bent character with increasing excitation of the anti-symmetric stretching vibration, it is more obvious to call it a "quasi-bent" molecule. By analogy, $\gamma_0 = -0.64$ is obtained when considering the (0, 1^1, 1) and (0, 2^0, 1) states.

The vibrational term energy, G_v, of a triatomic linear molecule can be expressed according to VPT2 by the equation

$$G_v = E_0 + \sum_i^3 \omega_i \left(v_i + \frac{d_i}{2}\right) + \sum_{i \le j}^3 x_{ij} \left(v_i + \frac{d_i}{2}\right)\left(v_j + \frac{d_j}{2}\right) + x_{\ell\ell}\ell^2, \tag{5}$$

where the indices i and j represent the vibrational modes of the molecule, x_{ij} are the anharmonicity parameters, and d_k is the degeneracy of the vibrational mode (1 for $k = \{1, 3\}$ and 2 for $k = \{2\}$). By subtracting appropriate VBOs, it is possible to obtain effective values for the anharmonicity parameters x_{ij} (details can be found in the supplementary material). The anharmonicity parameters x_{11}, x_{33}, and x_{13} can be calculated by combining the present experimental VBOs for band A, B, and C as well as the literature values for ν_1[22] and ν_3[27] yielding $x_{11} = -10.32$ cm^{-1}, $x_{33} = -13.68$ cm^{-1}, and $x_{13} = -4.38$ cm^{-1}. Employing the variational VBOs for the aforementioned bands yields almost identical values. However, by combining the theoretical VBOs for ν_1, ν_3, $2\nu_1$, and $2\nu_3$ as well as bands A and E, one arrives at a different set of x_{ij}: $x_{11} = -6.69$ cm^{-1}, $x_{33} = -23.45$ cm^{-1}, and $x_{13} = 0.34$ cm^{-1}. Finally, the VPT2 result employing the QFF of Table III is $x_{11} = -2.90$ cm^{-1},

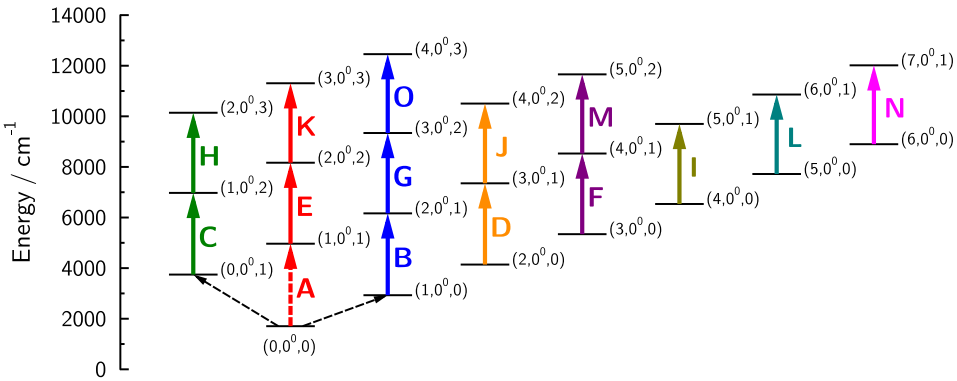

FIG. 11. Energy level scheme of observed stretching states in C_3, including the variationally calculated zero-point energy. For the series of bands originating from the (1, 0^0, 0) and (0, 0^0, 1) states, the lowest level is placed at the experimentally known term energy.[21,22] In the case of bands D, F, I, L, and N, the lower state term energy corresponds to the G_v of the present calculations: 2435.8, 3637.1, 4830.0, 6015.1, and 7192.9 cm^{-1}, respectively. The latter values are attributed a conservative error estimate of 3 cm^{-1}.

$x_{33} = -10.08$ cm^{-1}, and $x_{13} = -15.98$ cm^{-1}. The strong variation of the x_{ij} with the type of calculation used to obtain them shows that the underlying assumption of perturbation theory of any order, *i.e.* that is that perturbations are small compared to the zeroth order (harmonic) solution, is not fulfilled for C_3, and hence, Eq. (5) does not apply.

V. CONCLUSION

Fifteen combination bands of vibrationally excited gas-phase C_3 have been measured at high resolution; fourteen of which are reported for the first time. Figure 11 presents an energy level scheme of the detected vibrational states. Previously observed transitions are represented by dashed arrows. All term energies include the variationally calculated zero-point energy of 1705.06 cm^{-1} by Schröder and Sebald.[18] VBOs of the fifteen observed bands as well as rotational and centrifugal distortion parameters for all twenty-three involved states have been determined. The present variational ro-vibrational calculations of the stretching modes give remarkable agreement between experimental values and theoretical estimates; the typical accuracy of the rotational parameters is a few 0.001%. The experimental results offer a significant extension of the available data set for the C_3 molecule since they extend the observed number of quanta in both v_1 and v_3.

These highly excited vibrational states offer the best test of the reliability of the employed model in the calculations, as they should exhibit the greatest effect of the anharmonicity. Interestingly, the situation is somewhat reversed for C_3 compared to a well behaved molecule, as seen by the variation of the B_v values, where highly excited states show a more or less linear dependence on the vibrational quantum numbers, and the erratic behavior of the anharmonicity parameters obtained from *low* lying vibrational states. Clearly, the ro-vibrational spectrum of C_3 cannot be described by a theory based on a simple model like VPT2 even when a highly accurate PES is employed. However, using an accurate PES in conjunction with variational calculations employing the exact ro-vibrational Hamiltonian, it is possible to predict reliable line positions for this peculiar molecule.

SUPPLEMENTARY MATERIAL

See supplementary material for the complete line lists with observed-calculated values obtained from spectral fitting of the experimental spectrum using the PGOPHER software[40] for all fifteen bands (A–O). In addition, a detailed discussion on how the anharmonicity parameters are determined is given.

ACKNOWLEDGMENTS

The authors would like to thank the financial support of the Netherlands Organization for Scientific Research (NWO) through a VICI grant and the Netherlands Research School for Astronomy (NOVA). This study started many years ago, and at that time was in close collaboration with the late Peter Botschwina. On May 4th, he would have celebrated his 70th birthday. This paper is dedicated to him in memory of many years of intense collaborations.

[1] W. Huggins, Proc. R. Soc. London **33**, 1 (1881).
[2] A. McKellar, Astrophys. J. **108**, 453 (1948).
[3] R. G. W. Norrish, G. Porter, and B. A. Thrush, Proc. R. Soc. A **216**, 165 (1953).
[4] P. Swings, A. McKellar, and K. Narahari Rao, Mon. Not. R. Astron. Soc. **113**, 571 (1953).
[5] D. Crampton, A. P. Cowley, and R. M. Humphreys, Astrophys. J. Lett. **198**, L135 (1975).
[6] K. W. Hinkle, J. J. Keady, and P. F. Bernath, Science **241**, 1319 (1988).
[7] J. Cernicharo, J. R. Goicoechea, and E. Caux, Astrophys. J. Lett. **534**, L199 (2000).
[8] J. P. Maier, N. M. Lakin, G. A. H. Walker, and D. A. Bohlender, Astrophys. J. **553**, 267 (2001).
[9] T. Oka, J. A. Thorburn, B. J. McCall, S. D. Friedman, L. M. Hobbs, P. Sonnentrucker, D. E. Welty, and D. G. York, Astrophys. J. **582**, 823 (2003).
[10] B. Mookerjea, T. Giesen, J. Stutzki, J. Cernicharo, J. R. Goicoechea, M. De Luca, T. A. Bell, H. Gupta, M. Gerin, C. M. Persson, P. Sonnentrucker, Z. Makai, J. Black, F. Boulanger, A. Coutens, E. Dartois, P. Encrenaz, E. Falgarone, T. Geballe, B. Godard, P. F. Goldsmith, C. Gry, P. Hennebelle, E. Herbst, P. Hily-Blant, C. Joblin, M. Kaźmierczak, R. Kołos, J. Krełowski, D. C. Lis, J. Martin-Pintado, K. M. Menten, R. Monje, J. C. Pearson, M. Perault, T. G. Phillips, R. Plume, M. Salez, S. Schlemmer, M. Schmidt, D. Teyssier, C. Vastel, S. Yu, P. Dieleman, R. Güsten, C. E. Honingh, P. Morris, P. Roelfsema, R. Schieder, A. G. G. M. Tielens, and J. Zmuidzinas, Astron. Astrophys. **521**, L13 (2010).
[11] M. R. Schmidt, J. Krełowski, G. A. Galazutdinov, D. Zhao, M. A. Haddad, W. Ubachs, and H. Linnartz, Mon. Not. R. Astron. Soc. **441**, 1134 (2014).
[12] P. Botschwina, J. Phys. Chem. A **111**, 7431 (2007).
[13] C. A. Schmuttenmaer, R. C. Cohen, N. Pugliano, J. R. Heath, A. L. Cooksy, K. L. Busarow, and R. J. Saykally, Science **249**, 897 (1990).
[14] P. Jensen, C. M. Rohlfing, and J. Almlöf, J. Chem. Phys. **97**, 3399 (1992).
[15] M. Mladenović, S. Schmatz, and P. Botschwina, J. Chem. Phys. **101**, 5891 (1994).
[16] K. Ahmed, G. G. Balint-Kurti, and C. M. Western, J. Chem. Phys. **121**, 10041 (2004).
[17] C. M. R. Rocha and A. J. C. Varandas, J. Chem. Phys. **143**, 074302 (2015).
[18] B. Schröder and P. Sebald, J. Chem. Phys. **144**, 044307 (2016).

[19]A. E. Douglas, Astrophys. J. **114**, 466 (1951).
[20]L. Gausset, G. Herzberg, A. Lagerqvist, and B. Rosen, Astrophys. J. **142**, 45 (1965).
[21]K. Matsumura, H. Kanamori, K. Kawaguchi, and E. Hirota, J. Chem. Phys. **89**, 3491 (1988).
[22]G. Zhang, K.-S. Chen, A. J. Merer, Y.-C. Hsu, W.-J. Chen, S. Shaji, and Y.-A. Liao, J. Chem. Phys. **122**, 244308 (2005).
[23]A. A. Breier, T. Büchling, R. Schnierer, V. Lutter, G. W. Fuchs, K. M. T. Yamada, B. Mookerjea, J. Stutzki, and T. F. Giesen, J. Chem. Phys. **145**, 234302 (2016).
[24]J. Krieg, V. Lutter, C. P. Endres, I. H. Keppeler, P. Jensen, M. E. Harding, J. Vázquez, S. Schlemmer, T. F. Giesen, and S. Thorwirth, J. Phys. Chem. A **117**, 3332 (2013).
[25]W. Kraemer, P. Bunker, and M. Yoshimine, J. Mol. Spectrosc. **107**, 191 (1984).
[26]F. J. Northrup, T. J. Sears, and E. A. Rohlfing, J. Mol. Spectrosc. **145**, 74 (1991).
[27]K. Kawaguchi, K. Matsumura, H. Kanamori, and E. Hirota, J. Chem. Phys. **91**, 1953 (1989).
[28]F. J. Northrup and T. J. Sears, J. Opt. Soc. Am. B **7**, 1924 (1990).
[29]R. Gendriesch, K. Pehl, T. Giesen, G. Winnewisser, and I. Lewen, Z. Naturforsch. A **58**, 129 (2003).
[30]M. Haddad, D. Zhao, H. Linnartz, and W. Ubachs, J. Mol. Spectrosc. **297**, 41 (2014).
[31]D. Zhao, J. Guss, A. J. Walsh, and H. Linnartz, Chem. Phys. Lett. **565**, 132 (2013).
[32]D. Zhao, K. D. Doney, and H. Linnartz, Astrophys. J. Lett. **791**, L28 (2014).
[33]K. D. Doney, D. Zhao, and H. Linnartz, J. Mol. Spectrosc. **316**, 54 (2015).
[34]T. Motylewski and H. Linnartz, Rev. Sci. Instrum. **70**, 1305 (1999).
[35]G. Bazalgette Courrèges-Lacoste, J. P. Sprengers, J. Bulthuis, S. Stolte, T. Motylewski, and H. Linnartz, Chem. Phys. Lett. **335**, 209 (2001).
[36]G. Bazalgette Courrèges-Lacoste, J. P. Sprengers, W. Ubachs, S. Stolte, and H. Linnartz, J. Mol. Spectrosc. **205**, 341 (2001).
[37]L. Rothman, I. Gordon, Y. Babikov, A. Barbe, D. C. Benner, P. Bernath, M. Birk, L. Bizzocchi, V. Boudon, L. Brown, A. Campargue, K. Chance, E. Cohen, L. Coudert, V. Devi, B. Drouin, A. Fayt, J.-M. Flaud, R. Gamache, J. Harrison, J.-M. Hartmann, C. Hill, J. Hodges, D. Jacquemart, A. Jolly, J. Lamouroux, R. L. Roy, G. Li, D. Long, O. Lyulin, C. Mackie, S. Massie, S. Mikhailenko, H. Mijller, O. Naumenko, A. Nikitin, J. Orphal, V. Perevalov, A. Perrin, E. Polovtseva, C. Richard, M. Smith, E. Starikova, K. Sung, S. Tashkun, J. Tennyson, G. Toon, V. Tyuterev, and G. Wagner, J. Quant. Spectrosc. Radiat. Transfer **130**, 4 (2013).
[38]S. Carter and N. C. Handy, Mol. Phys. **57**, 175 (1986).
[39]P. Sebald, "*Ab initio* Berechnung spektroskopischer Eigenschaften kleiner linearer Moleküle," doctoral dissertation (University of Kaiserslautern, 1990).
[40]C. M. Western, PGOPHER version 8.0, University of Bristol Research Data Repository, 2014.
[41]D. Zhao, M. A. Haddad, H. Linnartz, and W. Ubachs, J. Chem. Phys. **135**, 044307 (2011).
[42]H. H. Nielsen, in *Encyclopedia of Physics*, edited by S. Flügge (Springer, Berlin, 1959), Vol. XXXVII/1 ATOMS III—MOLECULES I, p. 173.
[43]E. A. Rohlfing, J. Chem. Phys. **91**, 4531 (1989).
[44]K. Yamada and M. Winnewisser, Z. Naturforsch. A **31**, 139 (1976).